Materials Horizons

COMMUNICATION

View Article Online
View Journal | View Issue

Cite this: *Mater. Horiz.*, 2020, 7, 282

Received 23rd July 2019,
Accepted 5th September 2019

DOI: 10.1039/c9mh01148j

rsc.li/materials-horizons

A reversible underwater glue based on photo- and thermo-responsive dynamic covalent bonds†

Zhao Wang,[ab] Lifeng Guo,[ab] Hongyan Xiao,[a] Huan Cong *[ab] and Shutao Wang *[ab]

The intriguing reversible underwater adhesive phenomena in nature have inspired the rapid development of artificial adhesives by microscopic topography engineering or chemical modification on solid surfaces. However, most of the existing reversible underwater adhesives often suffer from low adhesion strength or complex fabrication processes. Here we present a reversible underwater glue by incorporating photo- and thermal-responsive anthracenyl moieties into an adhesive polyethylenimine backbone, featuring strong, widely tunable adhesion strength from 50.5 ± 7.4 to 606.7 ± 30.3 kPa, desirable fluidity, and compatibility to various substrates. Under orthogonal photo- and thermal stimuli, the reversible anthracene dimerization endows dynamic forming and breaking of cross-linked polymer networks within the glue, leading to reversible adhesion between solid substrates. Moreover, the glue can spontaneously spread over solid surfaces and absorb interfacial water molecules to realize adequate contact, promoting strong adhesion to diverse substrates and liquid environments. This study will provide an important strategy to develop the next generation of smart underwater adhesives.

New concepts

Reversible underwater adhesives have attracted much attention but are still in their infancy, with most designs solely focused on solid-state tape materials. These tapes generally rely on switching the complex interfacial interactions between the functional groups of the tape surface and the solid surface to control underwater adhesion, which often suffer from low adhesion strength and laborious pre-modifications of solid surfaces. Herein, by taking advantage of dynamic covalent bonds and a hygroscopic polymer backbone, we pioneer a reversible underwater glue – its reversibility can be readily realized by switching its well-controlled bulk strength within the glue. We show that the designed glue can rapidly respond to photo- and thermal stimuli, demonstrating strong and widely tunable adhesion strength from 50.5 ± 7.4 to 606.7 ± 30.3 kPa. Compared to solid-state tapes, the hygroscopic glue features desirable fluidity which can absorb interfacial water molecules to promote adequate contact and strong underwater adhesion to diverse substrates without any surface chemical and/or structural prefunctionalization. This design principle opens a new avenue for developing high-performance smart underwater adhesives, showing encouraging potential for intelligent wet/underwater transportation devices in industrial, military, and some other relevant fields.

1. Introduction

Underwater adhesives are highly desirable and indispensable materials in many fields including object transportation,[1] medical surgeries,[2] and stretchable electronics.[3] Inspired by wet and underwater adhesion in nature, such as toe pads of tree frogs,[4] suction cups of octopi,[5] hexagonal facets of clingfish,[6] and adhesive proteins of mussels,[7] significant progress has been made in artificial underwater adhesives through molecular design and structural engineering. Recently, reversible underwater adhesives have attracted particular attention owing to easy detachment from the bonded surfaces, which benefits the recyclability of both the adhesives and the substrates. However, reversible underwater adhesives are still in their infancy, with most designs focused on solid-state tapes. Examples include bio-inspired micro/nano-patterned tapes using weak interactions or suction stress,[8–14] polymer-grafted tapes using stimuli-responsive conformational changes,[15,16] and adhesive hydrogel tapes using host–guest interactions or dynamic covalent bonds.[17–24] Most of these reversible tape-like adhesives can easily attach onto and detach from solid surfaces, and their reversibility generally relies on the reversible interactions between functional groups of the tape surface and the solid surface. As another important form of underwater adhesive, liquid/viscous glues have aroused much attention because of their high adhesion strength, desirable fluidity, and broad applicable surfaces. These glues mostly function by incorporating catechol

[a] *Key Laboratory of Bio-inspired Materials and Interfacial Science, Key Laboratory of Photochemical Conversion and Optoelectronic Materials, Technical Institute of Physics and Chemistry, Chinese Academy of Sciences, Beijing 100190, P. R. China. E-mail: hcong@mail.ipc.ac.cn, stwang@mail.ipc.ac.cn*

[b] *School of Future Technology, University of Chinese Academy of Sciences, Beijing 100049, P. R. China*

† Electronic supplementary information (ESI) available. See DOI: 10.1039/c9mh01148j

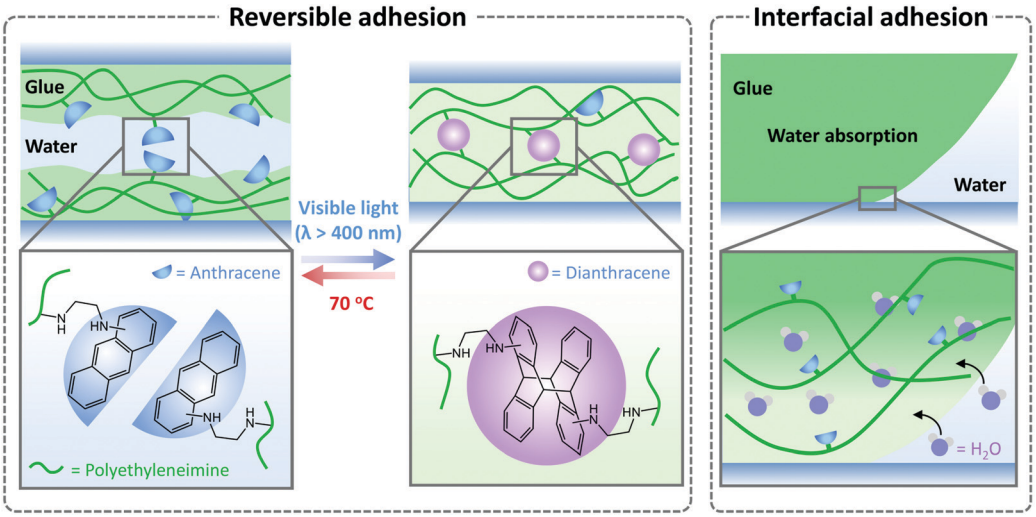

Fig. 1 Design of the anthracenyl-functionalized polyethylenimine (anth-PEI) as a reversible underwater glue. Due to the reversible crosslinking of anth-PEI networks, the glue can achieve switchable underwater adhesion under orthogonal physical stimuli. The hygroscopic and hydrophilic anth-PEI glue can spontaneously spread over the surfaces and absorb interfacial water, achieving effective interfacial adhesion.

or dopamine as adhesive groups into peptidomimetic polymers,[25–31] polyelectrolyte complexes[32–35] or supramolecular architectures,[36] and some physical mixture of gallol and/or tannic acid and polymers.[37,38] However, most of these glues irreversibly adhere onto the targeted substrates and are hard to separate on demand. Therefore, it remains a great challenge to fabricate underwater glues with reversible adhesion performance.

Herein, we report a reversible underwater glue composed of anthracenyl-functionalized polyethylenimine (anth-PEI) exhibiting strong and widely tunable adhesion based on dynamically covalent bonding in response to orthogonal photo- and thermal stimuli (Fig. 1). Taking advantage of the photo-induced anthracene [4+4] dimerization reaction,[39–42] formation of covalent bonds upon visible light irradiation could build crosslinked polymer networks, which dramatically enhance the underwater adhesion strength. While under elevated temperature, the cycloreversion of dianthracene would lead to crosslinking dissociation with concurrently reduced adhesion strength, thereby achieving reversible underwater adhesion. Polyethylenimine (PEI) was selected as the polymer backbone of the glue, because its hygroscopicity and hydrophilicity[43,44] can facilitate the absorbance of interfacial water molecules to strongly adhere onto the substrates. We envision that underwater glue with strong and switchable adhesion could be obtained by combining photo/thermo-responsive anthracene moieties and the hygroscopic polymer.

2. Results and discussion

Glue preparation and reversible underwater adhesion

The anth-PEI glue can be easily prepared through one-pot reductive amination reaction[45] starting from anthraldehyde and commercially available polyethylenimine with tetrabutylammonium borohydride as a reductant. To investigate the influence of the anthracenyl regioisomers on underwater adhesion performance, three kinds of anth-PEI glues were synthesized starting from 1-, 2-, and 9-anthraldehyde, respectively (Fig. 2a). Detailed synthesis and characterization information is provided in the ESI† (Fig. S1S3). The yellow viscous glues can be prepared on gram scales, thereby enabling batch adhesion testing. To evaluate the underwater adhesion properties, normalized testing samples were obtained by fixing two pieces of submerged quartz plates (with an overlapped area of 1 cm × 1 cm) employing anth-PEI glue, and then pressing the quartz plates with a preload before visible light irradiation using an LED blue light ($\lambda >$ 400 nm). The adhesion strength was measured on a tensile tester based on a lap normal joints model (Fig. S4, ESI†).[36]

The adhesion strength of 2-anth-PEI glue under otherwise identical conditions increased most quickly upon light irradiation likely due to the smallest steric hindrance, and reached a maximum of 381.0 ± 13.9 kPa after irradiation for 30 s (Fig. 2b). The adhesion strength of 9-anth-PEI glue gradually exceeded that of the 2-anth-PEI glue and the 1-anth-PEI glue after irradiation for 1 min. Further extending the irradiation time, the adhesion strength of 9-anth-PEI glue can reach its maximum of 606.7 ± 30.3 kPa at 2 min (Fig. 2c), and then remained almost unchanged (approx. 600 kPa). However, little change in the adhesion strength was observed in PEI networks upon irradiation. These results indicate that dimerization of the anthracene moieties can dramatically enhance the adhesion strength of anth-PEI glue by crosslinking polymer networks as monitored by UV-Vis measurements (Fig. S6a, ESI†).

We further evaluate the influence of anthracene content on underwater adhesion strength by incorporating different molar ratios of 9-anthracenyl into the PEI backbone (Fig. 2d). When the molar ratio of 9-anthracenyl to amino groups increased from 0 to 1.5%, the underwater adhesion strength after visible light irradiation surged from 68.7 ± 5.5 kPa to 606.7 ± 30.3 kPa (2 min irradiation time and 10 kPa preload), while further increasing the 9-anthracenyl content resulted in decreased

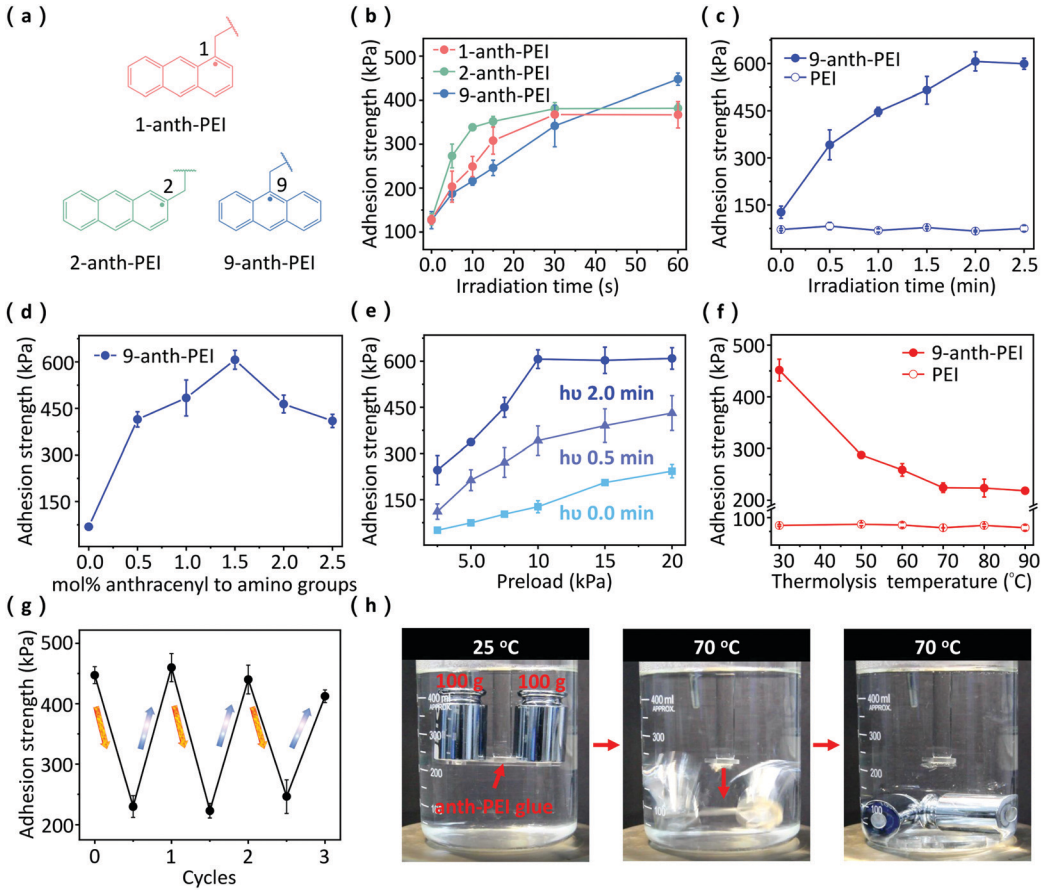

Fig. 2 Underwater adhesion performance of the anth-PEI glues. (a) Three kinds of anth-PEI glues with different anthracenyl regioisomers. (b) Underwater adhesion strength of anth-PEI glues influenced by anthracenyl regioisomers (1.5% molar ratio of anthracenyl to amino groups and 10 kPa preload). (c) Changes in underwater adhesion strength as a function of irradiation time (10 kPa preload). (d) Underwater adhesion strength with respect to molar ratios of 9-anthracenyl to amino groups (2 min irradiation time and 10 kPa preload). (e) Widely tunable underwater adhesion strength of 9-anth-PEI glue with different preloads and irradiation times. (f) Underwater adhesion strength as a function of thermolysis temperatures (15 min thermolysis time). (g) Reversible underwater adhesion of 9-anth-PEI glue upon alternating irradiation and heating. (h) The utility of 9-anth-PEI glue to control underwater adhesion strength (2 min irradiation time and 10 kPa preload).

adhesion strength. During the separation process of adhered substrates, the 9-anth-PEI glue all fractured in the bulk and remained intact at the contact interface between the glue and the substrate (Fig. S7, ESI†), indicating that bulk strength determines its maximal adhesion strength. A continuous increase of the anthracenyl incorporation ratio (>1.5 mol%) would weaken the bulk strength, thus resulting in decreased adhesion strength. In view of the highest adhesion strength, we chose the 9-anth-PEI glue with 1.5% anthracenyl incorporation ratio as the optimal glue for the subsequent research.

The above experiments were performed under a fixed preload of 10 kPa. It is well-known that adhesion strength highly depends on the applied preload through promoting good wettability of/contact to the substrate surfaces.[46] As expected, underwater adhesion strength could be further enhanced by increasing preloads under identical irradiation time (Fig. 2e). Without irradiation, the adhesion strength of 9-anth-PEI glue increased from 50.5 ± 7.4 to 242.8 ± 21.7 kPa as the applied preload increased from 2.5 to 20 kPa; upon irradiation, the variation trend in adhesion strength was consistent with that of non-irradiation and the adhesion strength can reach a maximum of 606.7 ± 30.3 kPa at 10 kPa preload after irradiation for 2 min. Therefore, a wide range of adhesion strength of 9-anth-PEI glue can be achieved from 50.5 ± 7.4 to 606.7 ± 30.3 kPa, indicating potential practical applications for different strength requirements.

We further investigated the reversibility of 9-anth-PEI glue by switching physical stimuli of irradiation and heating. Upon irradiation, the adhesion strength between the two quartz plates fixed by the glue can achieve 447.3 ± 14.0 kPa (10 kPa preload, Fig S5a, ESI†) after irradiation for 1 min. After heating the adhered glue for 15 min (Fig. S8 and S9, ESI†), the adhesion strength was significantly reduced with increasing thermolysis temperature (Fig. 2f and Fig. S5b, ESI†). Moreover, the reduced adhesion strength could be successfully recovered by subsequent light irradiation for 1 min (Fig. 2g). Upon repeatedly alternating irradiation and heating, 9-anth-PEI glue can maintain effective adhesion switching for at least 3 cycles. In contrast, the adhesion strength of PEI kept almost unchanged at approx. 70 kPa under different irradiation time and heating temperatures (Fig. 2c and f).

UV-Vis characterization during the reversible underwater adhesion process of 9-anth-PEI glue further evidenced the dynamic forming and breaking of covalent bonds between anthracenyl moieties (Fig. S6, ESI†). To further visualize the dramatic change of underwater adhesion strength, an underwater adhered sample with a 1 cm^2 adhesive area can hold 200 grams of weights after irradiation for 2 min, and detach on demand after heating at 70 °C (Fig. 2h).

Adhesion mechanism and compatibility

To understand the reversible underwater adhesion mechanism of 9-anth-PEI glue, we first investigated how contact was made between the glue and substrate. In an underwater environment, when a drop of 9-anth-PEI glue touched a glass surface, the aqueous layer quickly disappeared and a big dark spot emerged as observed by confocal laser scanning microscope (Fig. 3a). Upon irradiation, the storage moduli, loss moduli ($G' > G''$) and viscosity of the glue were increased owing to covalent crosslinking of anthracene moieties (Fig. 3c and Fig. S10, ESI†). As a result, the dark spot formed a stable state along with minimal spreading, indicating effective underwater adhesion. Without light irradiation, the dark spot gradually expanded over the entire substrate surface and in the meantime dissolved in water (Fig. 3b). In both cases, the 9-anth-PEI glue can achieve adequate contact with the substrate surface (Fig. S11, ESI†), which is a crucial step for underwater interfacial adhesion. We reasoned that the close contact between the 9-anth-PEI glue and the substrate should be related to the glue's ability for interfacial water absorption. Indeed, dynamic contact angle measurements revealed that a water droplet could be absorbed into a thin layer of glue-coating within 30 seconds (Fig. 3d and Fig. S12, ESI†), confirming good hygroscopicity of the 9-anth-PEI glue. In addition, we monitored the deadhesion process of a crosslinked 9-anth-PEI glue sample adhered to a glass substrate coated with an aqueous layer. When heated at 70 °C, the gel-like crosslinked glue was partly converted back into the fluidic viscous state over 10 min due to crosslinking dissociation, leading to gradual dissolution in water and separation from the substrate (Fig. 3e). The above results showed that combining the hygroscopic polymer backbone with photo/thermo-responsive anthracene moieties enables effective and reversible underwater adhesion.

Furthermore, 9-anth-PEI glue exhibits effective adhesion on a number of substrates with diverse surface charge and

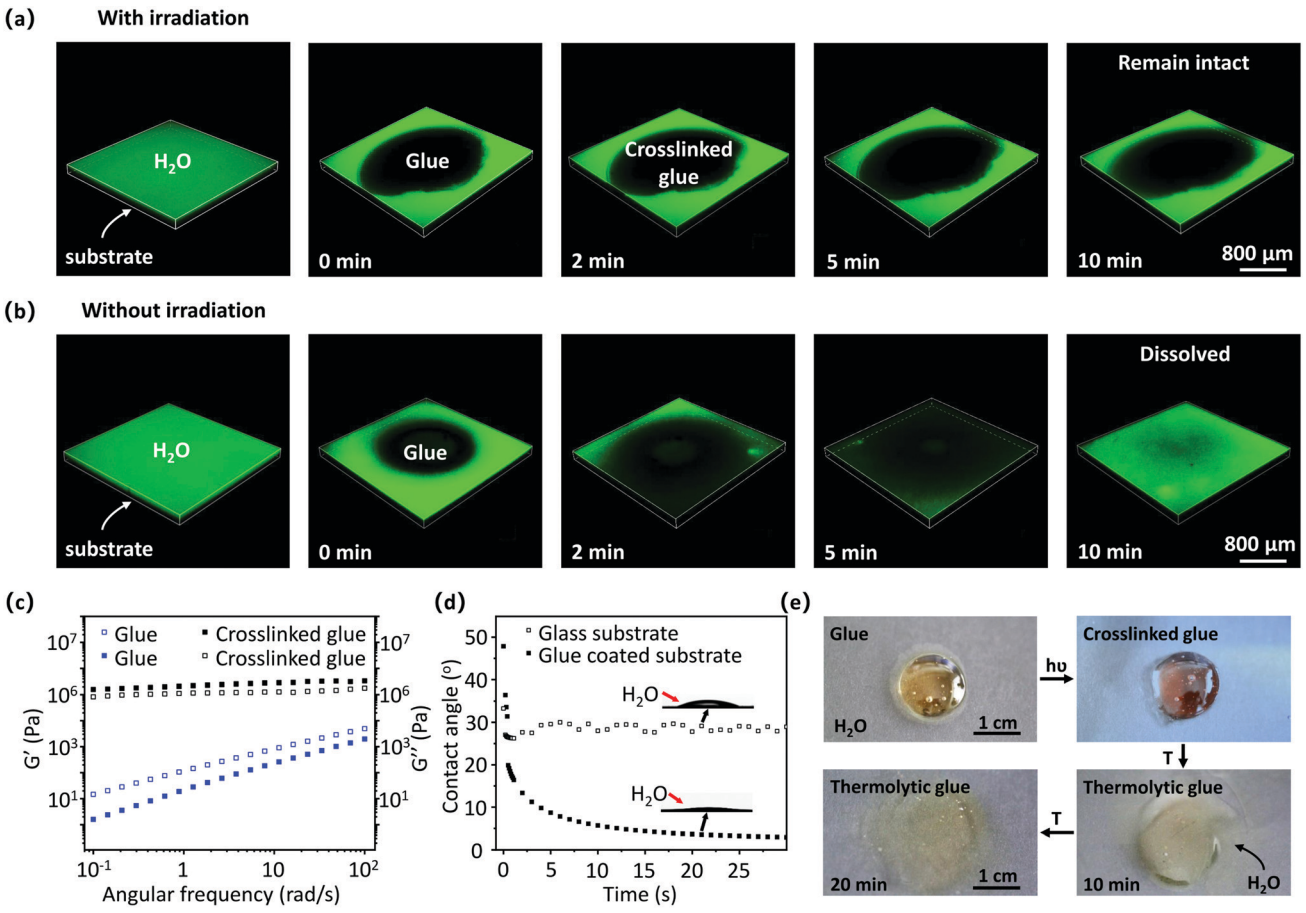

Fig. 3 Investigation of the mechanism for reversible underwater adhesion. Confocal images of (a) crosslinked 9-anth-PEI glue and (b) 9-anth-PEI glue in labeled water. (c) Frequency dependency of storage moduli G'(solid) and loss moduli G''(hollow) of 9-anth-PEI glue (blue) and crosslinked 9-anth-PEI glue (black). (d) The dynamic contact angles of a 9-anth-PEI glue coated substrate in comparison with a glass substrate. (e) The adhesion and deadhesion process of 9-anth-PEI glue on a water-coated quartz surface under physical stimuli.

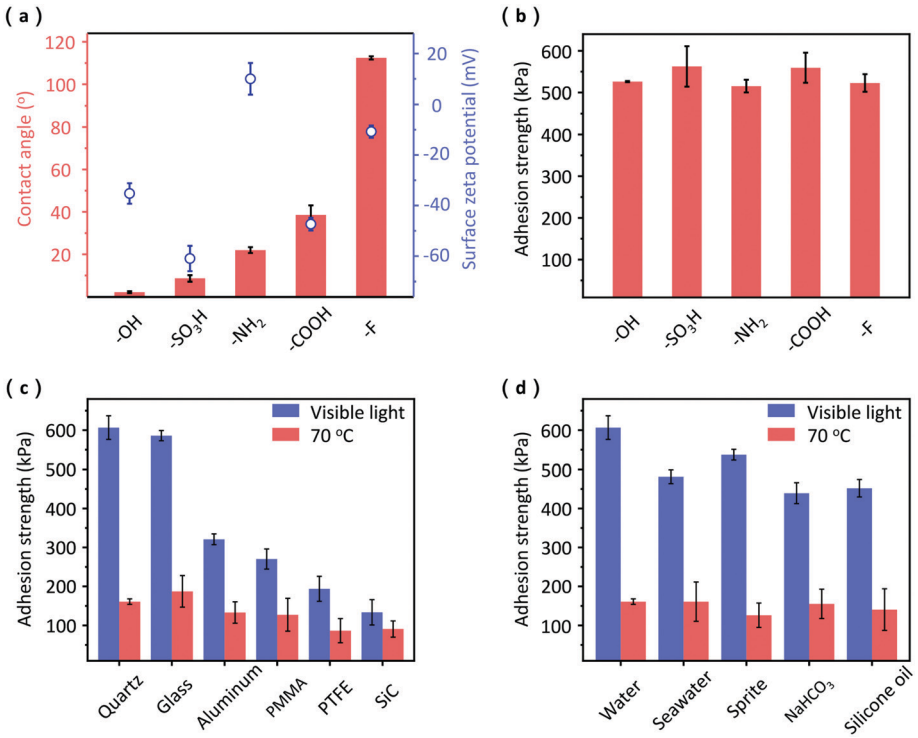

Fig. 4 Wide compatibility of 9-anth-PEI glue. (a) The contact angle and surface zeta potential of quartz surfaces with different grafting functional molecules. (b) High underwater adhesion strength on quartz surfaces with diverse charge and hydrophilicity (2 min irradiation time and 10 kPa preload). Tunable underwater adhesion occurs on different substrate surfaces (c) (5 min irradiation time and 10 kPa preload) and in diverse liquid environments (d) (2 min irradiation time and 10 kPa preload). PMMA polymethyl methacrylate, PTFE polytetrafluoroethylene, SiC silicon carbide.

hydrophilicity, suggesting broad potential applications. Surface modification with different functional molecules on quartz plates can vary the surface properties from positive charge ($-NH_3^+$) to negative charge ($-SO_3^-$), or from hydrophilic (–OH) to hydrophobic (–F) (Fig. 4a and Fig. S13, ESI†). The 9-anth-PEI glue can adhere to all of these modified surfaces with high adhesion strength (Fig. 4b). The switching adhesion of 9-anth-PEI glue can also be realized on a wide range of substrates, such

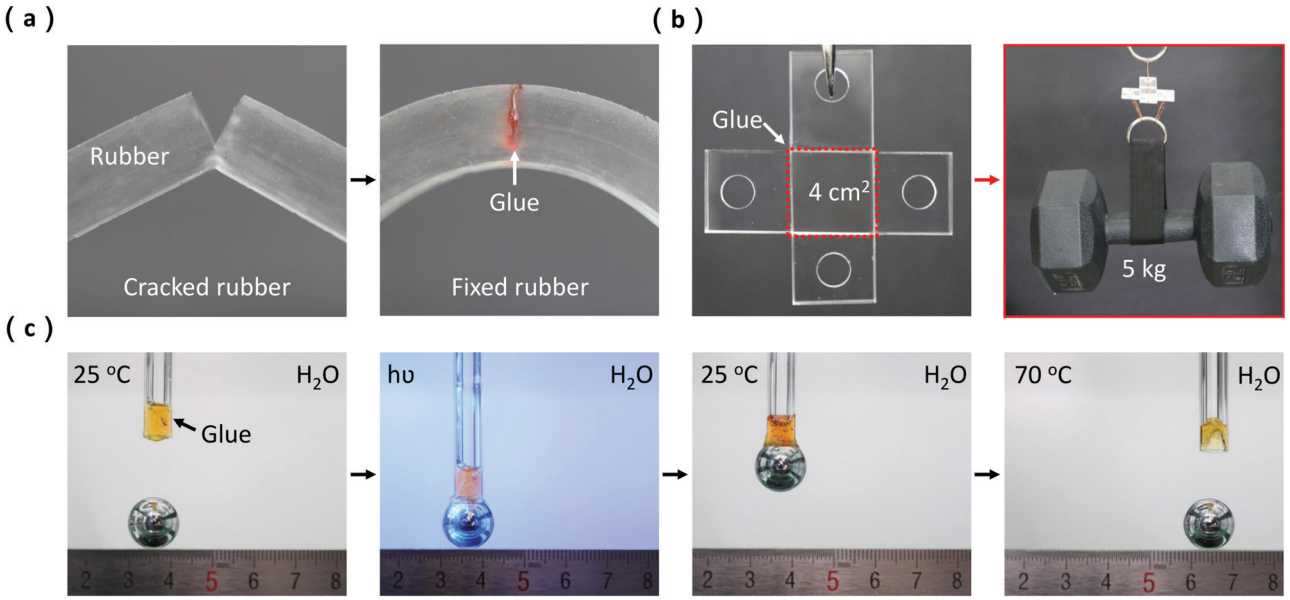

Fig. 5 Applications of 9-anth-PEI glue. (a) Precise adhesion of 9-anth-PEI glue on cracked silicone rubber surfaces after irradiation for 2 min. (b) An underwater adhered sample holding 5 kg of weight with a 4 cm^2 adhesive area. (c) Controllable underwater transport process of a steel ball using 9-anth-PEI glue.

as glass, metal, ceramic, and challenging smooth plastics with low surface energy (Fig. 4c and Fig. S14, ESI†). Besides, in diverse liquid environments such as sea water, Sprite (pH = 3.09), $NaHCO_3$ solution (pH = 8.05), and silicone oil, the 9-anth-PEI glue can show excellent switchable adhesive properties on quartz plates (Fig. 4d).

Applications of the 9-anth-PEI glue

One of the notable features of 9-anth-PEI glue is the desirable fluidic property, evidenced by the fact that its storage modulus (G') was less than the loss modulus (G'') in the frequency range from 0.1 to 100 rad s^{-1} (Fig. 3c). Such a feature enables 9-anth-PEI glue to achieve adequate contact and strong adhesion with rough, uneven substrate surfaces. For example, cracked silicone rubber can be fixed by the 9-anth-PEI glue after irradiation for 2 min along with recovered mechanical properties (Fig. 5a). To further visualize strong underwater adhesion, we showed that an underwater adhered sample with a 4 cm^2 adhesive area can hold at least 5 kg of weight after irradiation for 2 min (Fig. 5b). Moreover, the 9-anth-PEI glue can successfully capture and transfer a steel ball after visible light irradiation under water (Fig. 5c). When raising the temperature from 25 °C to 70 °C at a rate of around 5 °C min^{-1}, the steel ball can be further released after heating for *ca.* 12 min at *ca.* 70 °C in the bath (Fig. S15, ESI†), indicating the potential of the 9-anth-PEI glue for reversible capture and release of objects underwater.

3. Conclusions

We have demonstrated a photo- and thermal-responsive reversible underwater anth-PEI glue featuring strong, widely tunable adhesion strength from 50.5 ± 7.4 to 606.7 ± 30.3 kPa, desirable fluidity and versatility with various substrates and liquid environments. Moreover, the realization of strong underwater adhesion does not require any surface premodification. These attractive properties can be attributed to the design principle, namely, the use of reversible anthracene dimerization reaction to form a dynamic polymer network. This crosslinked network can respond to orthogonal physical stimuli, and the hydroscopic polyethylenimine can strongly stick to the substrate by absorbing interfacial water and providing abundant sources of electrostatic and hydrogen bond interactions. This study provides a unique design principle for reversible underwater adhesives – its reversibility relies on switching its well-controlled bulk strength but not the complex interfacial interactions between the glue and the solid surface. This design principle might be extended to other reversible underwater adhesives by introducing alternative stimuli-responsive molecules, such as azobenzene, spiropyrane and coumarin, or replacing PEI with other adhesive polymers. We believe that the reversible underwater glues will be promising for various important applications, such as transfer printing, bio-sensors, and smart bandages.

Conflicts of interest

There are no conflicts to declare.

Acknowledgements

Financial support from the Strategic Priority Research Program of the Chinese Academy of Sciences (XDB17000000), the National Key Research and Development Program of China (2017YFA0206903), the National Natural Science Foundation of China (21672227, 21425314, 21922113), National Program for Special Support of Eminent Professionals, the Recruitment Program of Global Experts, and K.C.Wong Education Foundation is gratefully acknowledged.

References

1 Y. Ma, S. Ma, Y. Wu, X. Pei, S. N. Gorb, Z. Wang, W. Liu and F. Zhou, *Adv. Mater.*, 2018, **30**, 1801595.
2 M. Shin, S. G. Park, B. C. Oh, K. Kim, S. Jo, M. S. Lee, S. S. Oh, S. H. Hong, E. C. Shin, K. S. Kim, S. W. Kang and H. Lee, *Nat. Mater.*, 2017, **16**, 147–152.
3 S. Baik, D. W. Kim, Y. Park, T. J. Lee, S. Ho Bhang and C. Pang, *Nature*, 2017, **546**, 396–400.
4 L. Xue, B. Sanz, A. Luo, K. T. Turner, X. Wang, D. Tan, R. Zhang, H. Du, M. Steinhart, C. Mijangos, M. Guttmann, M. Kappl and A. Del Campo, *ACS Nano*, 2017, **11**, 9711–9719.
5 F. Tramacere, E. Appel, B. Mazzolai and S. N. Gorb, *Beilstein J. Nanotechnol.*, 2014, **5**, 561–565.
6 P. Ditsche, D. K. Wainwright and A. P. Summers, *J. Exp. Biol.*, 2014, **217**, 2548–2554.
7 J. H. Waite, *J. Exp. Biol.*, 2017, **220**, 517–530.
8 H. Lee, B. P. Lee and P. B. Messersmith, *Nature*, 2007, **448**, 338–341.
9 P. Glass, H. Chung, N. R. Washburn and M. Sitti, *Langmuir*, 2010, **26**, 17357–17362.
10 D. M. Drotlef, P. Blumler and A. del Campo, *Adv. Mater.*, 2014, **26**, 775–779.
11 L. Xue, A. Kovalev, A. Eichler-Volf, M. Steinhart and S. N. Gorb, *Nat. Commun.*, 2015, **6**, 6621.
12 H. Lee, D.-S. Um, Y. Lee, S. Lim, H.-J. Kim and H. Ko, *Adv. Mater.*, 2016, **28**, 7457–7465.
13 R. Ping, S. T. Lin, C. Liang, T. Riku, S. Gento, G. Hui, K. D. R. K. Takayuki and G. J. Ping, *Adv. Mater.*, 2018, **30**, 1801884.
14 G. Ju, M. Cheng, F. Guo, Q. Zhang and F. Shi, *Angew. Chem., Int. Ed.*, 2018, **130**, 9101–9105.
15 Y. Ahn, Y. Jang, N. Selvapalam, G. Yun and K. Kim, *Angew. Chem., Int. Ed.*, 2013, **52**, 3140–3144.
16 Y. Zhao, Y. Wu, L. Wang, M. Zhang, X. Chen, M. Liu, J. Fan, J. Liu, F. Zhou and Z. Wang, *Nat. Commun.*, 2017, **8**, 2218.
17 Z. Shafiq, J. Cui, L. Pastor-Perez, V. San Miguel, R. A. Gropeanu, C. Serrano and A. del Campo, *Angew. Chem., Int. Ed.*, 2012, **51**, 4332–4335.
18 T. Nakamura, Y. Takashima, A. Hashidzume, H. Yamaguchi and A. Harada, *Nat. Commun.*, 2014, **5**, 4622.
19 A. R. Narkar, B. Barker, M. Clisch, J. Jiang and B. P. Lee, *Chem. Mater.*, 2016, **28**, 5432–5439.
20 J. Li, A. D. Celiz, J. Yang, Q. Yang, I. Wamala, W. Whyte, B. R. Seo, N. V. Vasilyev, J. J. Vlassak, Z. Suo and D. J. Mooney, *Science*, 2017, **357**, 378–381.

21 S. Ma, M. Scaraggi, P. Lin, B. Yu, D. Wang, D. Dini and F. Zhou, *J. Phys. Chem. C*, 2017, **121**, 8452–8463.
22 H. Yi, S. H. Lee, M. Seong, M. K. Kwak and H. E. Jeong, *J. Mater. Chem. B*, 2018, **6**, 8064–8070.
23 J. Liu, C. S. Y. Tan and O. A. Scherman, *Angew. Chem., Int. Ed.*, 2018, **57**, 8854–8858.
24 J. Yang, R. Bai and Z. Suo, *Adv. Mater.*, 2018, **30**, 1800671.
25 M. E. Yu and T. J. Deming, *Macromolecules*, 1998, **31**, 4739–4745.
26 M. J. Sever, J. T. Weisser, J. Monahan, S. Srinivasan and J. J. Wilker, *Angew. Chem., Int. Ed.*, 2004, **43**, 448–450.
27 J. D. White and J. J. Wilker, *Macromolecules*, 2011, **44**, 5085–5088.
28 B. Yang, N. Ayyadurai, H. Yun, Y. S. Choi, B. H. Hwang, J. Huang, Q. Lu, H. Zeng and H. J. Cha, *Angew. Chem., Int. Ed.*, 2014, **53**, 13360–13364.
29 J. Xu, X. Li, J. Li, X. Li, B. Li, Y. Wang, L. Wu and W. Li, *Angew. Chem., Int. Ed.*, 2017, **56**, 8731–8735.
30 C. J. Higginson, K. G. Malollari, Y. Xu, A. V. Kelleghan, N. G. Ricapito and P. Messersmith, *Angew. Chem., Int. Ed.*, 2019, **35**, 12271–12279.
31 A. Cholewinski, F. Yang and B. Zhao, *Mater. Horiz.*, 2019, **6**, 285–293.
32 H. Shao and R. J. Stewart, *Adv. Mater.*, 2010, **22**, 729–733.
33 B. K. Ahn, S. Das, R. Linstadt, Y. Kaufman, N. R. Martinez-Rodriguez, R. Mirshafian, E. Kesselman, Y. Talmon, B. H. Lipshutz, J. N. Israelachvili and J. H. Waite, *Nat. Commun.*, 2015, **6**, 8663.
34 Q. Zhao, D. W. Lee, B. K. Ahn, S. Seo, Y. Kaufman, J. N. Israelachvili and J. H. Waite, *Nat. Mater.*, 2016, **15**, 407–412.
35 M. Dompé, F. J. Cedano-Serrano, O. Heckert, N. van den Heuvel, J. van der Gucht, Y. Tran, D. Hourdet, C. Creton and M. Kamperman, *Adv. Mater.*, 2019, **31**, 1808179.
36 A. H. Hofman, I. A. van Hees, J. Yang and M. Kamperman, *Adv. Mater.*, 2018, **30**, 1704640.
37 K. Kim, M. Shin, M.-Y. Koh, J. H. Ryu, M. S. Lee, S. Hong and H. Lee, *Adv. Funct. Mater.*, 2015, **25**, 2402–2410.
38 M. Shin, K. Kim, W. Shim, J. W. Yang and H. Lee, *ACS Biomater. Sci. Eng.*, 2016, **2**, 687–696.
39 T. Yamamoto, S. Yagyu and Y. Tezuka, *J. Am. Chem. Soc.*, 2016, **138**, 3904–3911.
40 Z.-A. Huang, C. Chen, X.-D. Yang, X.-B. Fan, W. Zhou, C.-H. Tung, L.-Z. Wu and H. Cong, *J. Am. Chem. Soc.*, 2016, **138**, 11144–11147.
41 T. Harper, R. Slegeris, I. Pramudya and H. Chung, *ACS Appl. Mater. Interfaces*, 2017, **9**, 1830–1839.
42 S. Kaiser, S. Radl, J. Manhart, S. Ayalur-Karunakaran, T. Griesser, A. Moser, C. Ganser, C. Teichert, W. Kern and S. Schlogl, *Soft Matter*, 2018, **14**, 2547–2559.
43 J. Bandrup, E. H. Immergut and E. A. Grulke, *Polymer Handbook*, Wiley, New York, 4th edn, 1999.
44 R. Tanaka, I. Ueoka, Y. Takaki, K. Kataoka and S. Saito, *Macromolecules*, 1983, **16**, 849–853.
45 A. F. AbdelMagid, K. G. Carson, B. D. Harris, C. A. Maryanoff and R. D. Shah, *J. Org. Chem.*, 1996, **61**, 3849–3862.
46 Q. Lin, D. Gourdon, C. Sun, N. Holten-Andersen, T. H. Anderson, J. H. Waite and J. N. Israelachvili, *Proc. Natl. Acad. Sci. U. S. A.*, 2007, **104**, 3782–3786.

